

Journal of Water and Wastewater, Vol. 31, No. 6, pp: 1-11

Kinetics and Adsorption Investigation of Malachite Green onto Thiolated Graphene Oxide Nanostructures

S. Salamat¹, E. Mohammadnia¹, M. Hadavifar²

1. Graduated Student, Dept. of Environmental Sciences,
Hakim Sabzevari University, Sabzevar, Iran

2. Assist. Prof., Dept. of Environmental Sciences,
Hakim Sabzevari University, Sabzevar, Iran

(Corresponding Author) mhadavifar@yahoo.com - m.hadavifar@hsu.ac.ir

(Received Nov. 8, 2019 Accepted Feb. 6, 2020)

To cite this article:

Salamat, S., Mohammadnia, E., Hadavifar, M. 2021. "Kinetics and adsorption investigation of malachite green onto thiolated graphene oxide nanostructures" Journal of Water and Wastewater, 31(6), 1-11.

Doi: 10.22093/wwj.2020.208052.2951.

Abstract

Release of dye-containing wastewater into ecosystems has posed serious risks to the environment and aquatic life because of toxicity and adverse effects on the water bodies. Malachite green is a basic dye that has very wide industrial applications, especially in the aquaculture industry. This study was carried out in order to remove the malachite green from aqueous solutions by thiolated graphene oxide in batch system. In the present work, the effects of experimental parameters such as adsorbent dosage, solution pH, initial dye concentration, thermodynamics and adsorption mechanism were comprehensively studied in batch system. In order to characterize the physical and chemical properties of the synthesized nanostructure and also to confirm the functionalization steps, different analyses including SEM and FT-IR were used. Batch studies showed that the experimental data fitted logically to applied isotherms, namely Langmuir ($R^2=0.991$) and Freundlich ($R^2=0.983$) models. Kinetic calculations confirmed that malachite green adsorption was described more accurately by pseudo-second order model compared to the pseudo-first order model. The study showed that thiolated graphene oxide is an effective adsorbent for malachite green removal from aqueous solution. Under controlled reaction conditions, Gibbs free energy (ΔG) varied from -1.46 to -3.25 kJ/mol, besides, the resulting ΔH° and ΔS° values were obtained 0.059 kJ/mol and 15.67 kJ/mol.K, respectively. So, it can be considered that the adsorption of malachite green onto the thiolated graphene oxide nanostructure is a physico-chemical and spontaneous process.

Keywords: Graphene Oxide, Malachite Green, Thiol Functional Group, Isotherm Models, Adsorption kinetics, Thermodynamics.



1. Introduction

The damages caused by industrial activities and technological advances are increasing and high remediation costs are needed. One of the problems of the twenty-first century that threatens the future of human life on this planet is the water scarcity problem. In the last decade, especially in the late twentieth century, water has been the focus of international debates (Salman, 2018). Pollution of aquatic ecosystems by dyeing wastewaters is one of the major environmental problems of the present century (Contreras et al., 2012).

Coloring wastewater produced by various industries including textile, paper, rubber and plastic. If these wastewaters are discharged to the environment they can cause significant environmental problems (Sadeghi-Kiakhani et al., 2013). Since dyes contain a complex aromatic molecular structure, they are important sources of water pollution due to their stability, visibility and resistance to biodegradability. The toxic effects of dyes on living cells occur when they selectively react with biomolecules such as glutathione, cysteine, homocysteine resulting in disruption of protein synthesis, disruption of enzyme activity and dysfunction (Srivastava et al., 2004).

Pigments cause many health problems, including skin allergy, skin irritation, cancer and genetic mutation (Gomez et al., 2007). Green malachite dye is one of the cationic dyes that is widely used in dyeing wool, silk, yarn, leather, paper and acrylic. Green malachite with the chemical formula $C_{23}H_{25}ClN_2$ is one of the most effective products in the control of foreign fungi and protozoa infecting fish. The use of green malachite causes direct damages such as carcinogenicity, mutagenicity and reduced fertility and indirect damages such as environmental problems and the natural cycles. In the year 2000, the use of green malachite was forbidden for eatable fish because the people who used it were exposed to the effects of malachite such as carcinogenesis and mutagenesis (Hameed and El-Khaiary, 2008).

Malachite Green is an aniline colored by-product and is known as an anomalous and fluctuating material. Green malachite, alone or in combination with formalin, is used as a fungus in monthly breeding (Raval et al., 2017). It is dangerous for mammals in the concentration of 0.1 $\mu\text{g/L}$ (Panandiker et al., 1992). Colored wastewater usually contains contaminants such as acids, bases, soluble solids, toxic compounds and dyes that are significant even in very small amounts and must be removed prior to discharging the wastewater into the water bodies (Kobyas et al., 2006).

Various technologies are available for the removal of malachite green dyes, including chemical composition, coagulation, membrane separation, ion exchange, photo oxidation, reverse osmosis and adsorption process (Mohammadnia et al., 2019, Salamat

et al., 2019). Adsorption is a process by which compounds in a solution are adsorbed onto an adsorbing material. The adsorption process has a high efficiency compared to other purification processes and is able to eliminate higher concentrations with lower cost (Tchobanoglous and Burton, 1991). Adsorbents such as carbon nanotubes (Ghasemi et al., 2019), Magnetic core-zeolitic shell (Padervand and Gholami, 2013), multiwall carbon nanotubes (MWCNTs) (Dehghani et al., 2015), nanoparticles and nanocomposites (Sarkhosh et al., 2016), BiOCl/AgCl-BiOI/AgI (Padervand et al., 2019) and graphene nanostructures (Mohammadnia et al., 2018) were used to remove various contaminants from water and wastewater. Graphene oxide (GO) is a layer of carbon atoms arranged with the SP^2 hybrid in a honeycomb and two-dimensional crystalline lattice that was first synthesized in 2004. Given the unique geometrical structure of this material, graphene can be expected to have remarkable physical and chemical properties including: high Young's modulus, high fracture toughness, excellent thermal and electrical conductivity, rapid mobility of loads, large surface area, bioavailability and high compatibility (Liu et al., 2013).

On a graphene plate, each carbon atom has a free bond off the plate. This bond is a suitable site for the incorporation of some functional groups as well as hydrogen atoms (Mohammadnia et al., 2019). The presence of heavy oxygen, hydroxyl, epoxide and carboxyl groups on graphene oxide plates provides a wide surface that can be used to remove metals and materials from wastewater (Han et al., 2012). The disadvantages of natural graphene are its incompatibility with organic polymers that cannot form a homogeneous composite. But this problem can be solved by functionalizing graphene layers. Graphene oxide has a high ability to be functionalized and so many materials are used for graphene functionalization such as iron, silica and chitosan. According to the above mentioned properties of graphene and its derivatives it can be considered as an effective adsorbent to remove substances from water (Wang et al., 2010). Therefore, in this study, we tried to increase the adsorbent surface and removal efficiency by using thiol functional groups, as well as by magnetizing the adsorbent to provide economical use of the adsorbent.

2. Materials and methods

2.1. Functionalizing of GO nanoparticles

2.1.1. GO/Fe₃O₄ preparation

Graphene oxide was provided by the modified Hummer method. The applied chemicals as potassium hydroxide, sodium hydroxide, nitric acid (65%), acetic acid, malachite green, $FeCl_2 \cdot 4H_2O$, $FeCl_3 \cdot 6H_2O$, ammonia solution and 3-Mercaptopropyltrimethoxysilane were prepared from Merck.

Initially, 0.1 g of graphene, 1 g of $FeCl_2 \cdot 4H_2O$ and



2.37 g of $\text{FeCl}_3 \cdot 6\text{H}_2\text{O}$ were mixed in 140 ml of water. The procedure was performed by adding 10 ml of 28% ammonia solution at 60 °C for 60 min. The black $\text{GO}/\text{Fe}_3\text{O}_4$ nanoparticles were separated with an external magnet, washed with water to neutral pH, and then dried at room temperature for 24 h.

2.1.2. Preparation of $\text{GO}/\text{Fe}_3\text{O}_4\text{-Si-Pr-SH}$

To prepare $\text{GO}/\text{Fe}_3\text{O}_4\text{-SH}$ nanoparticles, 0.5 g of $\text{GO}/\text{Fe}_3\text{O}_4$ nanoparticles was added to 50 ml of toluene containing 2 mmol of 3-Mercaptopropyltrimethoxysilane and the resulting mixture was refluxed for 24 h at 60 °C. The compound was then cooled to room temperature and filtered by an external magnet, and the product was washed with ethanol to remove any impurities and dried at 50 °C for 12 h, resulting in a powder mixture (Mohammadnia et al., 2019). FT-IR infrared spectroscopy was used to investigate the functional groups present in the adsorbent and SEM was used to investigate the surface structure of the adsorbent. Fig. 1 shows the schematic of the functionalization process of graphene nanoparticles.

2.2. Batch adsorption experiments

The removal of malachite green from aqueous solutions in a batch system conducted in a 250 mL container with a working volume of 100 mL. Initially, the malachite green stock solution was prepared at a concentration of 500 mg/L, and the required different concentrations of malachite green were prepared daily by dilution with distilled water. To optimize the adsorption process, initially, a certain dose of adsorbent (300, 500, 700 and 900 mg/L) was investigated under constant pH conditions, initial dye concentration and ambient temperature (25 °C). After determining the optimum adsorbent, the pH of the solution was adjusted 4 to 8, by adding 0.1 M HNO_3 and 0.1 M NaOH . Then, the effect of the dye concentration on adsorption process was investigated by changing the initial concentration of malachite.

The equilibrium study was performed by sampling at 0 to 60 min intervals. To evaluate isotherm studies, 4 solutions were prepared at concentrations of 10, 20, 30 and 40 mg/L of malachite green at pH 7 and in a constant dose of adsorbent (500mg/L). After 60 min (equilibrium time) sampling was performed and equilibrium concentration (C_e) was measured. The concentration of malachite green in solution was determined by spectrophotometric method at 620 nm (Salamat et al., 2019) and three replicates for each sample. The calibration curve applied for malachite green determination is as shown in Fig. 2. In every experiment, adsorbent efficiency was measured in two ways: equilibrium adsorption capacity (q_e) in mg/g and removal percentage (%R). q_e and %R were calculated

according to the Eq. (1) and Eq. (2), respectively (Hadavifar et al., 2016)

$$q_e = \frac{V}{M} (C_0 - C_e) \quad (1)$$

$$\%R = 100 \times \frac{V(C_0 - C_e)}{C_0} \quad (2)$$

$$q_e = \frac{q_m bc_e}{1 + bc_e} \quad (3)$$

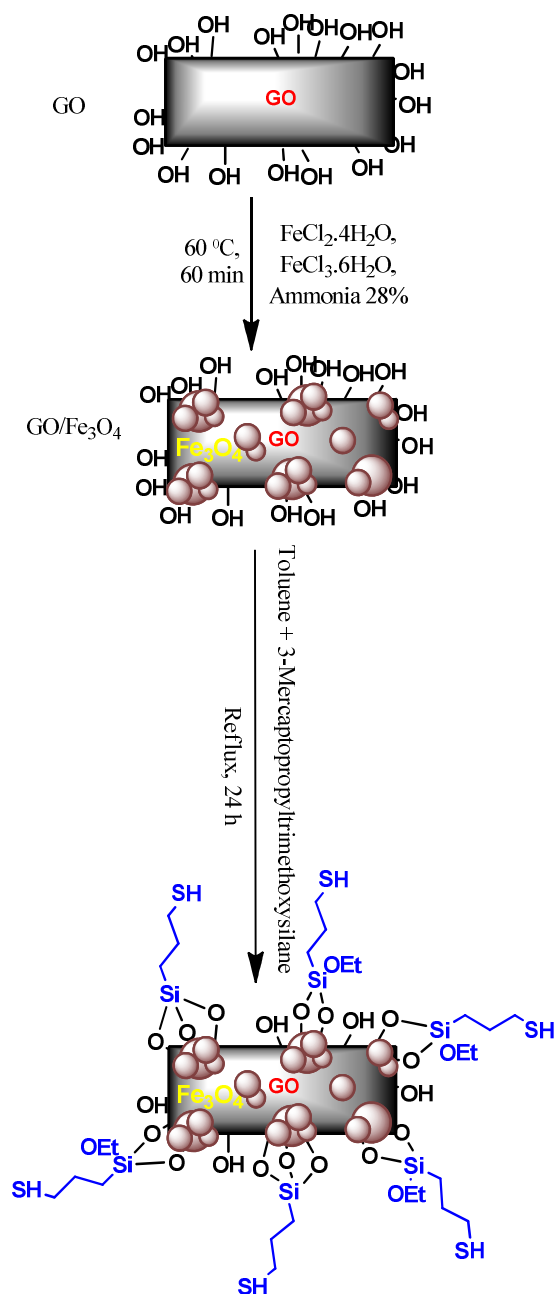


Fig. 1. Schematic of the functionalization of $\text{GO}/\text{Fe}_3\text{O}_4\text{-Si-Pr-SH}$ nanoparticles

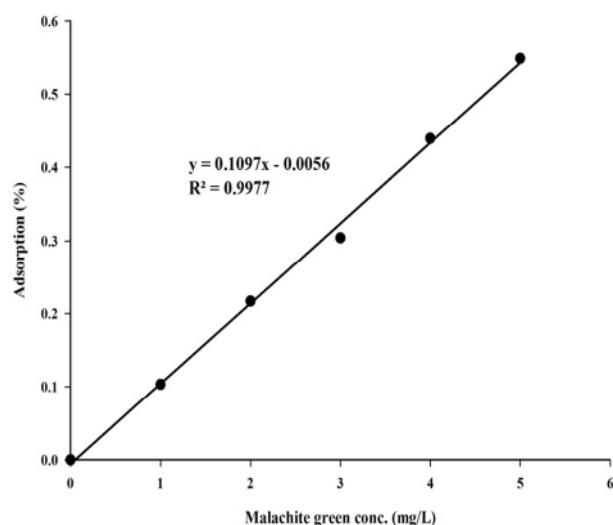


Fig. 2. The calibration curve for malachite green determination

2.3. Evaluation of adsorption process in batch system

The Langmuir and Freundlich isotherm models are widely used to determine the interaction between adsorbed dye molecules and residual dye molecules in the solution (Mohammadnia et al., 2018). The Langmuir and Freundlich models are explained by Eq. (3) and Eq. (4), respectively

$$q_e = K_f C_e^{1/n} \quad (4)$$

Where

q_e is the adsorption capacity of the adsorbent in mg/L and C_e is the dye concentration in mg/L at equilibrium time. The q_m is the maximum adsorption capacity of the adsorbent in mg/g, and b a constant in L/mg.

K_f is a constant related to the adsorption capacity of the adsorbent in $\text{mg/g} \cdot (\text{L/mg})^{1/n}$ and n is a dimensionless empirical constant presenting the intensity of adsorption. In fact, the greater the value of n is, the better its adsorption capacity (Hadavifar et al., 2016). The nonlinear regression analysis of isotherm models was done with SigmaPlot software (SigmaPlot 10.0, USA).

Dubinin-Radushkevich isotherm generally implies the adsorption mechanism with Gaussian energy distribution on a heterogeneous surface; its nonlinear form is presented as Eq. (5)

$$q_e = q_m \exp(-KE^2) \quad (5)$$

Where

E is adsorption energy (kJ/mol) that can be calculated by

$$E = RT \ln \left(1 + \frac{1}{C_e} \right) \quad \text{or} \quad E = (2K)^{\frac{1}{2}}, \quad K \text{ (mol.kJ)}^2 \text{ is}$$

Dubinin-Radushkevich isotherm constant, $R=8.314$ J/mol/K is the gas universal constant and T (K) is temperature.

2.4. Kinetic studies

To determine the adsorption kinetics of malachite onto the prepared adsorbent, Pseudo-first-order and pseudo-second-order kinetic models were used. The pseudo-first-order linear form is shown in Eq. (6) (Mohammadnia et al., 2019)

$$\text{Log}(q_e - q_t) = \text{Log}q_e - \frac{K_1}{2.303} t \quad (6)$$

The pseudo-second-order kinetics indicates chemical absorption. This model was suggested by Ho in 1995 as Eq. (7) (Ghasemi et al., 2019)

$$q_t = \frac{q_e^2 k_2 t}{q_e K_2 t + 1} \quad (7)$$

Where

q_e (mg/g) and q_t (mg/g) are the amount of adsorbed material at the equilibrium time and time t , respectively. k_1 (1/min) and k_2 (g/mg.min) are reaction rate constants of pseudo-first-order and pseudo-second-order kinetic models, respectively.

2.5. Thermodynamics

Other parameters affecting the adsorption rate are the ambient temperature of the process. To investigate the effect of temperature on the adsorption rate, the adsorption process of malachite green at 15, 25, 35 and 45 °C was investigated. The temperature was adjusted by incubator shaker. The other parameters were considered as dye concentration of 10 mg/L, 500 mg/L adsorbent dose and pH=7. Investigation of thermodynamic parameters requires determination of temperature distribution coefficient K . This coefficient is calculated from Eq. (8)

$$K_d = \frac{C_0 - C_e}{C_e} \times \frac{V}{W} \quad (8)$$

V (L) is working volume and W (g) is adsorbent weight. Other thermodynamic parameters of Gibbs free energy (ΔG°), enthalpy (ΔH°) and entropy (ΔS°) were determined by Eq. (9) and Eq. (10) (Farghali et al., 2013)

$$\text{Ln}K_d = \frac{\Delta S}{R} \times \frac{\Delta H}{RT} \quad (9)$$



$$\Delta G = \Delta H - T\Delta \quad (10)$$

Where

$R=8.314$ J/mol/K is gas universal constant and T (K) is temperature. ΔH° (J/mol) and ΔS° (J/mol/K) are respectively equal to slope and y-intercept of Van't Hoff fitted graph ($\text{Ln}K_d$ vs. $1/T$).

3. Results and Discussion

3.1. Physical and chemical properties of the functionalized GO

3.1.1. FT-IR spectroscopy

According to Fig. 3 the identification of the functional groups in raw and functionalized graphene oxide by FT-IR spectra was performed in the wavelength range of $400\text{--}4000\text{ cm}^{-1}$. In FT-IR spectra, as can be seen, the peak at the 582 cm^{-1} region is related to stretching bond of Fe-O and confirms the presence of Fe_3O_4 in the synthesized adsorbent. These peaks usually appear below 700 cm^{-1} and are attributed to changes in oxygen and iron bonding at the positions of their atomic sites (Santos et al., 2016, Mohammadnia et al., 2019).

In the graphene oxide spectrum before and after the functionalization, the peak at 1047.32 cm^{-1} is related to C-O adsorption zone (ester groups) and the peak at 3419.47 cm^{-1} is related to tensile vibrations of O-H bond (hydroxyl group) (Heidarpour et al., 2020), the width and the asymmetry of this peak indicate strong hydrogen bonds. The adsorption of C-H bond (alkanes group) occurs at 2974.47 cm^{-1} . In the GO, the peak at 1729.75 cm^{-1} is related to the tensile bond of C=O and 1625.66 cm^{-1} is related to the C=C bond (Pavia et al., 2008). The peak in the thiol-coated graphene oxide in the region of 2626.32 cm^{-1} is most likely related to the S-H bond vibration (Li et al., 2015). Comparison of the three spectra showed the successful functionalization of the adsorbent.

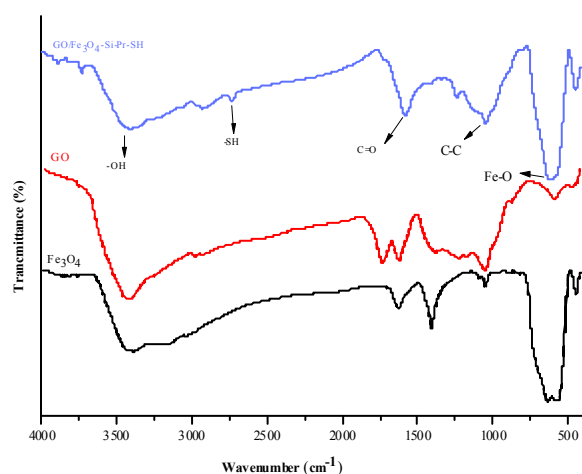


Fig. 3. FTIR spectra of GO, $\text{GO}/\text{Fe}_3\text{O}_4$, $\text{GO}/\text{Fe}_3\text{O}_4\text{-Si-Pr-SH}$ nanoparticles

3.1.2. SEM observations

The image of the scanning electron microscope (SEM) analysis for the synthesized adsorbent ($\text{GO}/\text{Fe}_3\text{O}_4\text{-Si-Pr-SH}$) is shown in Fig. 4. In principle, scanning electron microscopy images are used to study any disruption in the nanoparticle structure of bulk samples at or near the surface. The results of scanning electron microscopy show that the magnetic iron oxide particles have a good distribution on the graphene oxide plates. As shown in Fig. 4, the lighter phases are related to the magnetic nanoparticles and the darker phases to the carbon particles, which is due to the atomic number difference as the heavier phases have more electron reversibility (Hadavifar et al., 2016, Koju et al., 2018, Mohammadnia et al., 2019).

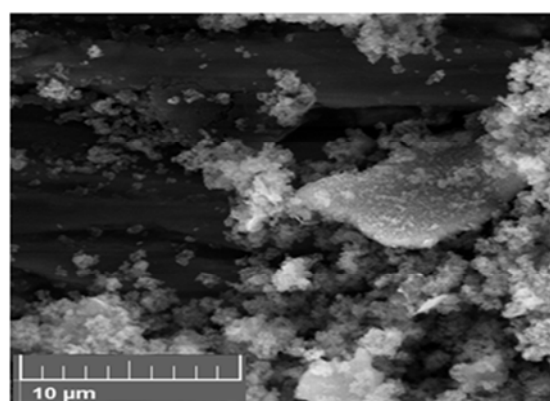


Fig. 4. SEM image of $\text{GO}/\text{Fe}_3\text{O}_4\text{-Si-Pr-SH}$ nanoparticles

3.2. Malachite green adsorption in batch system

3.2.1. The effect of adsorbent dosage

Various amounts of adsorbent (0.02 to 0.09 g/L) under ambient temperature, initial concentration of 10 mg/L, pH 7 and contact time of 60 min were used to evaluate the adsorbent concentration. According to Fig. 5, by increasing the adsorbent dose from 0.02 to 0.09 g/L, the removal percentage of malachite green was increased to

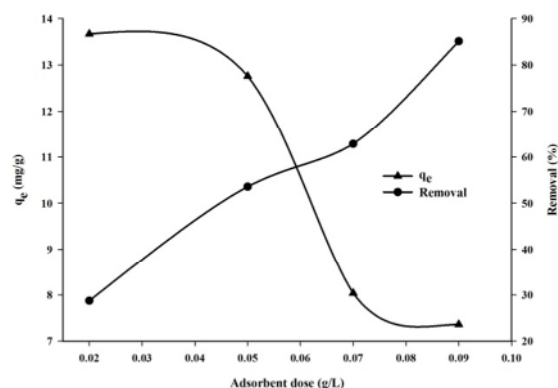


Fig. 5. Effect of adsorbent dosage on malachite green adsorption by $\text{GO}/\text{Fe}_3\text{O}_4\text{-Si-Pr-SH}$ nanoparticles (malachite green initial concentration: 10 mg/L, equilibrium time: 60 min and pH=7)



85% and the equilibrium adsorption capacity was reduced.

An increase in the percentage of malachite green removal can be due to the presence of free adsorption sites and an increase in the adsorbent surface (Dehghani et al., 2015). By increasing the adsorbent dose, it is possible to bond malachite cations with the negative charges on the adsorbent surface more closely. Increasing the number of these collisions between the adsorbate molecules and the adsorbent surface increases the adsorption of malachite from the aqueous solution and increases the adsorption efficiency (Porkodi and Kumar, 2007). On the other hand, increasing the adsorbent dose increases the free functional groups that do not bond to malachite green and, as a result, the adsorption capacity decreases.

3.2.2. The influence of pH on the adsorption process

The pH of solution plays an important role in the adsorption process affecting on other factors such as adsorbent surface charge, ionization of functional groups presenting on the active site of the adsorbent surface (Ribeiro et al., 2012). The aqueous solution pH is one of the most important control parameters of the adsorption process, because the bonding of cations to the surface groups is strongly dependent on the surface charge of the particles (Ngomsik et al., 2012). According to Fig. 6, with increase in the pH, the removal rate of malachite green increased to pH 7, achieving a higher removal value of 73%.

In fact, at higher pH, the adsorbent surface may be more negatively charged (due to OH⁻ ions) which increases the electrostatic scattering between the dye cations and the adsorbent surface (Srivastava et al., 2004). At acidic pH, the number of H⁺ ions increases in the media and competes with malachite green dye as a cationic dye. This can reduce the adsorption of malachite green (Mall et al., 2005). On the other hand, with

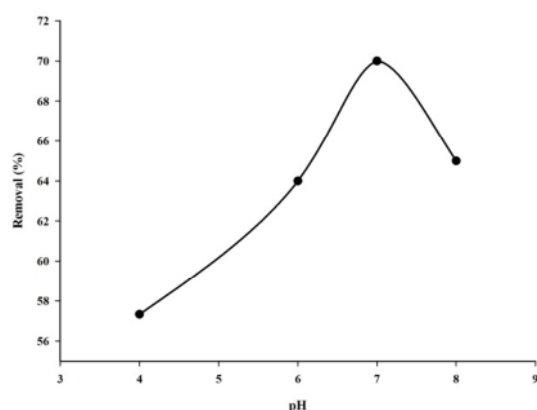


Fig. 6. Effect of pH on malachite green adsorption onto GO/Fe₃O₄-Si-Pr-SH nanoparticles (malachite green initial concentration: 10 mg/L, adsorbent dosage: 0.05 g/L, equilibrium time: 60 min)

increasing the pH from 4 to 7, the competition between H⁺ ions and cationic ions of malachite green decreases and malachite green mainly occupies adsorbent sites. Studies have shown that at higher pH values, malachite discoloration increases due to the reaction of its double bonds with OH⁻ (Chen and Elimelech, 2008, Lu et al., 2009). So, experiments were performed at optimum pH of 7 to prevent the hydrolysis of malachite green dye.

3.2.3. The effect of concentration on the adsorption process

The concentration of adsorbate is one of the factors affecting on the adsorption process. According to Fig. 7, the highest percentage removal was obtained at 10 mg/L and the lowest at 40 mg/L of malachite green concentrations.

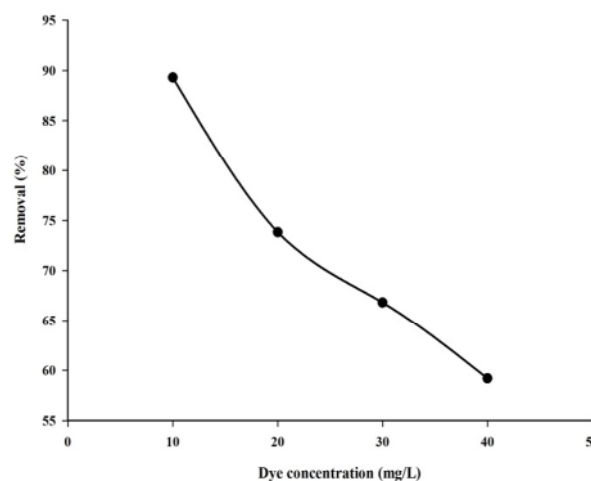


Fig. 7. Effect of initial concentration on malachite green adsorption onto GO/Fe₃O₄-Si-Pr-SH nanoparticles (adsorbent dosage: 0.01 g/L, equilibrium time: 60 min and pH=7)

The decrease in the adsorption percentage with increasing concentration may be attributed to the constant number of active sites on the adsorbent compared to increasing adsorbate molecules (Han et al., 2007, Hadavifar et al., 2014). On the other hand, by increasing the initial dye concentration, it is possible that the repulsive force between adsorbate molecules occurs, preventing them from bonding to the adsorbent surface (Crini and Badot, 2008).

3.2.4. Effect of contact time on the adsorption process

The adsorption of malachite green was performed for 120 min and sampling was done at 10, 20, 30, 40, 60, 80, 100 and 120 minute intervals to investigate the adsorption process over time. Fig. 8 illustrates the effect of time on the adsorption process under constant conditions (pH=7, adsorbent dose 0.03 g/L and dye concentration of 10 mg/L).



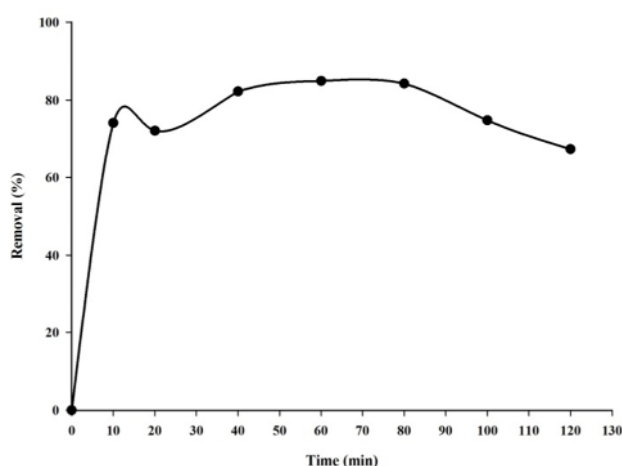


Fig. 8. Effect of contact time on malachite green adsorption onto GO/Fe₃O₄-Si-Pr-SH (adsorbent dosage: 0.05 g/L, malachite green initial concentration: 10 mg/L, equilibrium time: 120 min and pH=7)

As can be seen, the highest removal occurred in the first 10 min and then the adsorption increased slowly until reaching equilibrium in 60 min and then decreased due to desorption. Over time, the active sites were gradually occupied on the adsorbent surface leading to the desorption of malachite green from the adsorbent surface, so the adsorption removal was reduced (Shirsath and Shirivastava, 2015). However, changing the solution pH over time may be effective on the desorption process.

3.2.5. Adsorption isotherm

The adsorption isotherms explain how the adsorbed materials interact with the adsorbent providing a comprehensive understanding of the nature of the adsorption process (Dehghani et al., 2015). The adsorption isotherms indicate the relationship between the amount of adsorbed molecules at the constant temperature and equilibrium concentration in the solution. As a single operation, physico-chemical adsorption trend was also determined using obtained data from these isotherm models to evaluate the applicability of the adsorption process (Lim et al., 2018). To obtain information about the absorption trend, the data were fitted to three Langmuir, Freundlich and Dubinin-Radushkevich isotherm models. According to the Fig. 9 and correlation coefficient values presented in Table 1, it is clear that in all three Langmuir ($R^2 = 0.991$), Freundlich ($R^2 = 0.983$) and Dubinin-Radushkevich models ($R^2 = 0.96$) the obtained R^2 values logically describe the goodness of fitting trend.

According to the obtained results, in Langmuir model the adsorption process occurred uniformly and on a homogeneous surface as an adsorption monolayer without adsorbed molecules interaction. The b parameter (mg/L) is the equilibrium constant which refers to the bond formation energy of the adsorption process, which

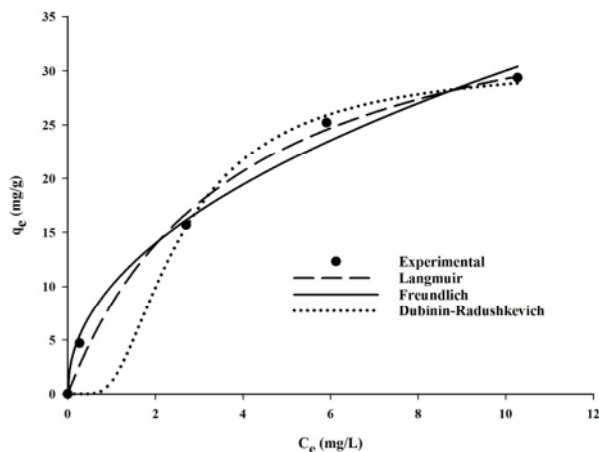


Fig. 9. Adsorption isotherm of malachite green onto GO/Fe₃O₄-Si-Pr-SH at initial concentration of 10 to 50 mg/L, adsorbent dose of 0.05 g/L, pH 7 and temperature of 25 °C for 60 min

indicates the adsorption desirability, and its value was 0.26 for malachite green indicating a relatively strong bond with the adsorbent surface. In Freundlich model it is assumed that the multilayer adsorption occurs with a non-uniform energy distribution of the adsorption sites as well as with the interference of adsorbed ions (Sağ and Aktay, 2001). The parameters of K_f and n are the constants of this model which reflect the absorption capacity and intensity, respectively (Vazquez et al., 2002). Values of $1/n$ between 0 and 1 indicate the heterogeneity of the adsorbent. Obtained K_f value was $10.06 \text{ mg/g} \cdot (\text{L/mg})^{1/n}$ for malachite green and 0.47 for $1/n$, indicating that the adsorption capacity and heterogeneity of the adsorbent are favorable (Shirsath and Shirivastava, 2015). The Dubinin-Radushkevich model generally refers to the expression of the adsorption mechanism by the Gaussian energy distribution on a heterogeneous surface. Where parameter E (kJ/mol) represents the average absorption energy indicating the type of adsorption; this value for malachite green was 0.04 kJ/mol.

3.2.6. Adsorption kinetics

In order to investigate the factors affecting the reaction rate, it is necessary to study the process kinetics. Therefore, in the present study, pseudo-first-order and pseudo-second-order kinetic models for malachite green adsorption were investigated. Since the data did not match logically, the pseudo-first-order results have not been shown. According to Table 2, the parameters of the pseudo-second-order model and its correlation coefficients showed that the pseudo-second-order kinetic equation provides a good fitness of the data (Fig. 10).

The pseudo-first-order equation describes the adsorption in solid-solution systems based on the solids adsorption capacity, while the pseudo-second-order

Table 1. Langmuir, Freundlich and Dubinin–Radushkevich parameters for adsorption of malachite green onto GO/Fe₃O₄-Si-Pr-SH

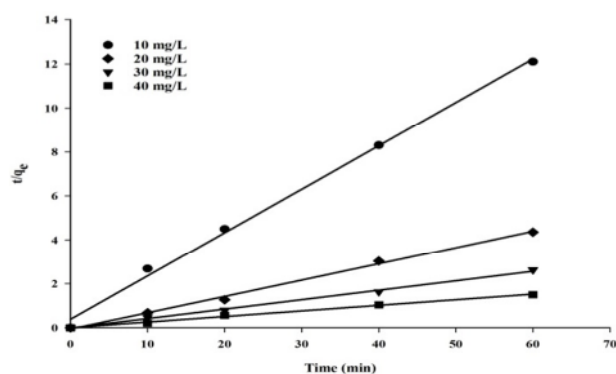
Langmuir			Freundlich			Dubinin–Radushkevich		
q _m (mg/g)	b (l/mg)	R ²	K _f	1/n	R ²	q _m (mg/g)	E (kJ/mol)	R ²
40.5	0.26	0.991	10.06	0.47	0.983	6.38	0.04	0.96

Table 2. Kinetic adsorption parameters obtained using pseudo-second-order models

Malachite green conc. (mg/L)	q _{e,exp}	Pseudo-second-order		
		K ₂ (g/mg.min)	q _{e2} (mg/g)	R ²
10	4.7	0.02892	5.06	0.997
20	15.68	0.00550	13.47	0.996
30	25.23	0.00184	23.31	0.995
40	29.36	0.00064	39.37	0.996

Table 3. Thermodynamic parameters of malachite green adsorption onto GO/Fe₃O₄-Si-Pr-SH

ΔS° (kJ/mol.K)	ΔH° (kJ/mol)	Temperature (K)	288	298	308	318	R ²
15.67	0.059	ΔG° (kJ/mol)	-1.46	-2.06	-2.66	-3.25	0.91

**Fig. 10.** Pseudo-second-order of malachite green adsorption onto GO/Fe₃O₄-Si-Pr-SH

equation is used to analyze the chemical kinetics of liquid solutions (Porkodi and Kumar, 2007). This equation shows that the chemical adsorption is the deceleration step of the adsorption rate. In this model, the adsorption process is due to the physical and chemical interactions between the two solid and soluble phases (Vazquez et al., 2002). The best adsorption model was obtained from the experimental data based on the R² correlation coefficient and comparing the q values. The pseudo-second-order model with R² value of 0.99 and also the similarity of the adsorption capacity obtained from this model with the adsorption capacity obtained from the experimental calculations showed that it was in good agreement.

On the other hand, by increasing the concentration from 10 to 50 mg/L, the graph slopes are reduced and constant values of the pseudo-second order equation (K₂) are decreasing throughout the process, indicating a rapid

saturation of active sites adsorbed by malachite green molecules (Srivastava et al., 2008). These results indicate that the process of removal of malachite green follows the pseudo-second-order kinetics and according to a good fitness by the Langmuir isothermal model it can be concluded that the adsorption process was monolayer and a dominant and controlling mechanism in the adsorption process was chemical adsorption.

3.2.7. Effect of temperature and adsorption thermodynamics

In order to study the effect of temperature on the adsorption of malachite green onto the graphene oxide nanoparticles, thermodynamic studies were conducted at adsorbent dose of 0.03 g/L, pH 7, initial dye concentration of 10 mg/L and four different temperatures of 20, 30, 40 and 15 °C. According to the results, the obtained ΔG values show the influence of temperature on the adsorption process of malachite onto graphene oxide nanoparticles surface by Ln K_d linear diagram against 1/T as shown in Fig. 11. Also, the obtained thermodynamic parameters and their calculated correlation coefficients are given in Table 3. Under constant reaction conditions, Gibbs free energy (ΔG) varied from -1.46 to -3.25 kJ/mol, and the resulting ΔH° and ΔS° values were obtained 0.059 kJ/mol and 15.67 kJ/mol.K, respectively. Positive values of ΔH° as well as the increasing trend of K_d with increasing temperature indicate that the adsorption of malachite green on the surface of thiolated graphene oxide nanoparticles is endothermic. In endothermic reactions, if the temperature is increased, the amount of TΔS° (favorable factor) also is increased and TΔS° acts as a favorable reaction agent. This means that as the temperature

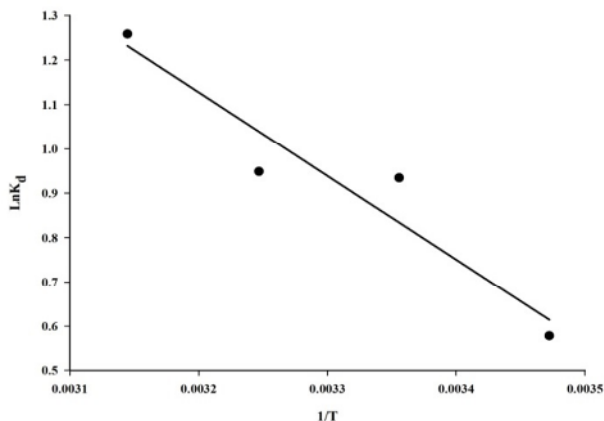


Fig. 11. Plots of $\ln K_d$ versus $1/T$ for malachite green adsorption onto GO/Fe₃O₄-Si-Pr-SH (adsorbent dose of 0.05 g/L, pH 7.0 and initial malachite green concentration of 10 mg/L)

increases, the adsorption rate also increases (Ghasemi et al., 2019). This enhanced temperature provides the energy needed for dehydration of dye molecules and the breakage of hydrogen bonds between the water molecules and the adsorbent surface leading to increase in surface active sites (Shahbazi et al., 2013). Molecules adsorption on a smaller than the chemical reactions that are very specific. The value of ΔG° in physical temperature data of the model showed that both monolayer adsorption, which represents chemical adsorption, and multilayer adsorption, which reflects a physical adsorption, occurred during this process. From this perspective, it can be assumed that the adsorption of absorption varies between 0 and -20 kJ/mol. However, in chemical and physical absorption this rate varies

between -20 to -80 kJ/mol and -80 to 80 kJ/mol (Ghasemi et al., 2019). In addition, according to the malachite green on the surface of thiolated graphene oxide nanoparticles it can occur both physically and chemically which is in agreement with the data of the isotherm models.

4. Conclusions

In the present work, thiolated graphene oxide was used to remove malachite green dye from aqueous solutions. The results of the SEM and FT-IR analyses showed that the synthesis of thiolated graphene oxide was carried out successfully. The results showed that all applied isotherm models logically described the adsorption process. The maximum malachite green adsorption capacity was predicted as 40.5 mg/g by Langmuir model. The kinetic studies revealed that the pseudo-first-order model did not fit with the experimental data and pseudo-second-order kinetic model was fitted logically to the experimental data.

The results of this research also revealed that the Gibbs free energy (ΔG) varied from -1.46 to -3.25 kJ/mol, and the resulting ΔH° and ΔS° values were obtained 0.059 kJ/mol and 15.67 kJ/mol.K, respectively, representing that both physical and chemical adsorption of malachite green on the surface of thiolated graphene oxide nanoparticles can occur, which is in agreement with the data obtained from the isothermal models.

5. Acknowledgements

The authors appreciate the sponsorship of the Ministry of Science, Research and Technology of Iran, and the financial support of the Hakim Sabzevari University and Iran Nanotechnology Initiative Council.

References

- Chen, K. L. & Elimelech, M. 2008. Interaction of fullerene (C60) nanoparticles with humic acid and alginate coated silica surfaces: measurements, mechanisms, and environmental implications. *Environmental Science and Technology*, 42(20), 7607-7614.
- Contreras, E., Sepúlveda, L. & Palma, C. 2012. Valorization of agroindustrial wastes as biosorbent for the removal of textile dyes from aqueous solutions. *International Journal of Chemical Engineering*, 679352.
- Crini, G. & Badot, P. M. 2008. Application of chitosan, a natural aminopolysaccharide, for dye removal from aqueous solutions by adsorption processes using batch studies: a review of recent literature. *Progress in Polymer Science*, 33(4), 399-447.
- Dehghani, M. H., Taher, M. M., Bajpai, A. K., Heibati, B., Tyagi, I., Asif, M. et al. 2015. Removal of noxious Cr (VI) ions using single-walled carbon nanotubes and multi-walled carbon nanotubes. *Chemical Engineering Journal*, 279, 344-352.
- Farghali, A. Bahgat, M., Eirouby, W. M. & Khedr, M. H. 2013. Decoration of multi-walled carbon nanotubes (MWCNTs) with different ferrite nanoparticles and its use as an adsorbent. *Journal of Nanostructure in Chemistry*, 3(1), 50.
- Ghasemi, S. S., Hadavifar, M., Maleki, B. & Mohammadnia, E. 2019. Adsorption of mercury ions from synthetic aqueous solution using polydopamine decorated SWCNTs. *Journal of Water Process Engineering*,



- 32, 100965.
- Gomez, V., Larrechi, M. S. & Callao, M. P. 2007. Kinetic and adsorption study of acid dye removal using activated carbon. *Chemosphere*, 69(7), 1151-1158.
- Hadavifar, M., Bahramifar, N., Younesi, H. & Li, Q. 2014. Adsorption of mercury ions from synthetic and real wastewater aqueous solution by functionalized multi-walled carbon nanotube with both amino and thiolated groups. *Chemical Engineering Journal*, 237, 217-228.
- Hadavifar, M., Bahramifar, N., Younesi, H., Rastakhiz, M., Li, Q., Yu, J. et al. 2016. Removal of mercury(II) and cadmium(II) ions from synthetic wastewater by a newly synthesized amino and thiolated multi-walled carbon nanotubes. *Journal of the Taiwan Institute of Chemical Engineers*, 67, 397-405.
- Hameed, B. H. & El-Khaiary, M. I. 2008. Equilibrium, kinetics and mechanism of malachite green adsorption on activated carbon prepared from bamboo by K_2CO_3 activation and subsequent gasification with CO_2 . *Journal of Hazardous Materials*, 157(2-3), 344-351.
- Han, Q., Wang, Z., Xia, J., Chen, S., Zhang, X. & Ding, M. 2012. Facile and tunable fabrication of Fe_3O_4 /graphene oxide nanocomposites and their application in the magnetic solid-phase extraction of polycyclic aromatic hydrocarbons from environmental water samples. *Talanta*, 101, 388-395.
- Han, R., Wang, Y., Yu, W., Zou, W., Shi, J. & Liu, H. 2007. Biosorption of methylene blue from aqueous solution by rice husk in a fixed-bed column. *Journal of Hazardous Materials*, 141(3), 713-718.
- Heidarpour, H., Padervand, M., Soltanieh, M. & Vossoughi, M. 2020. Enhanced decolorization of rhodamine B solution through simultaneous photocatalysis and persulfate activation over Fe/C_3N_4 photocatalyst. *Chemical Engineering Research and Design*, 153, 709-720.
- Kobyas, M., Demirbas, E., Can, O. T. & Bayramoglu, M. 2006. Treatment of levafix orange textile dye solution by electrocoagulation. *Journal of Hazardous Materials*, 132(2-3), 183-188.
- Koju, N. K., Song, X., Wang, Q., Hu, Z. & Colombo, C. 2018. Cadmium removal from simulated groundwater using alumina nanoparticles: behaviors and mechanisms. *Environmental Pollution*, 240, 255-266.
- Li, X., Zhou, H., Wu, W., Wei, S., Xu, Y. & Kuang, Y. 2015. Studies of heavy metal ion adsorption on Chitosan/Sulfdryl-functionalized graphene oxide composites. *Journal of Colloid and Interface Science*, 448, 389-397.
- Lim, J. Y., Mubarak, N. M., Abdullah, E. C., Nizamuddin, S. & Khalid, M. 2018. Recent trends in the synthesis of graphene and graphene oxide based nanomaterials for removal of heavy metals-a review. *Journal of Industrial and Engineering Chemistry*, 66, 29-44.
- Liu, J., Cui, L. & Losic, D. 2013. Graphene and graphene oxide as new nanocarriers for drug delivery applications. *Acta Biomaterialia*, 9(12), 9243-9257.
- Lu, J., Li, Y., Yan, X., Shi, B., Wang, D. & Tang, H. 2009. Sorption of atrazine onto humic acids (HAs) coated nanoparticles. *Colloids and Surfaces A: Physicochemical and Engineering Aspects*, 347(1), 90-96.
- Mall, I. D., Srivastava, V. C., Agarwal, N. K., Mishra & I. M. 2005. Adsorptive removal of malachite green dye from aqueous solution by bagasse fly ash and activated carbon-kinetic study and equilibrium isotherm analyses. *Colloids and Surfaces A: Physicochemical and Engineering Aspects*, 264(1-3), 17-28.
- Mohammadnia, E., Hadavifar, M. & Veisi, H. 2019. Kinetics and thermodynamics of mercury adsorption onto thiolated graphene oxide nanoparticles. *Polyhedron*, 173, 114139.
- Mohammadnia, E., Hadavifar, M. & Veisi, H. 2018. Adsorption of Cadmium (II) onto thiolated graphene oxide and kinetic investigations, *Amirkabir Journal of Civil Engineering*. doi: 10.22060/ceej.2018.14660.5710. (In Persian).
- Ngomsik, A. F., Bee, A., Talbot, D. & Cote, G. 2012. Magnetic solid-liquid extraction of Eu (III), La (III), Ni (II) and Co (II) with maghemite nanoparticles. *Separation and Purification Technology*, 86, 1-8.
- Padervand, M., Jalilian, E., Majdani, R. & Goshadezahn, M. 2019. BiOCl/AgCl-BiOI/AgI quaternary nanocomposite for the efficient photodegradation of organic wastewaters and pathogenic bacteria under visible light. *Journal of Water Process Engineering*, 29, 100789.
- Padervand, M. & Gholami, M. R. 2013. Removal of toxic heavy metal ions from waste water by functionalized



- magnetic core–zeolitic shell nanocomposites as adsorbents. *Environmental Science and Pollution Research*, 20(6), 3900-3909.
- Panandiker, A., Fernandes, C. & Rao, K. V. K. 1992. The cytotoxic properties of malachite green are associated with the increased demethylase, aryl hydrocarbon hydroxylase and lipid peroxidation in primary cultures of Syrian hamster embryo cells. *Cancer Letters*, 67(2), 93-101.
- Pavia, D. L., Lampman, G. M., Kriz, G. S. & Vyvyan, J. A. 2008. *Introduction to Spectroscopy*. Cengage Learning. Stanord, USA.
- Porkodi, K. & Kumar, K. V. 2007. Equilibrium, kinetics and mechanism modeling and simulation of basic and acid dyes sorption onto jute fiber carbon: eosin yellow, malachite green and crystal violet single component systems. *Journal of Hazardous Materials*, 143(1-2), 311-327.
- Raval, N. P., Shah, P. U. & Shah, N. K. 2017. Malachite green “a cationic dye” and its removal from aqueous solution by adsorption. *Applied Water Science*, 7(7), 3407-3445.
- Ribeiro, R. S., Fathy, N. A., Attia, A. A., Silva, A. M. T., Faria, J. L. & Gomes, H. T. 2012. Activated carbon xerogels for the removal of the anionic azo dyes Orange II and Chromotrope 2R by adsorption and catalytic wet peroxide oxidation. *Chemical Engineering Journal*, 195, 112-121.
- Sadeghi-Kiakhani, M., Arami, M. & Gharanjig, K. 2013. Preparation of chitosan-ethyl acrylate as a biopolymer adsorbent for basic dyes removal from colored solutions. *Journal of Environmental Chemical Engineering*, 1(3), 406-415.
- Sağ, Y. & Aktay, Y. 2001. Application of equilibrium and mass transfer models to dynamic removal of Cr(VI) ions by Chitin in packed column reactor. *Process Biochemistry*, 36(12), 1187-1197.
- Salamat, S., Hadavifar, M. & Rezaei, H. 2019. Preparation of nanochitosan-STP from shrimp shell and its application in removing of malachite green from aqueous solutions. *Journal of Environmental Chemical Engineering*, 7(5), 103328.
- Salman, M. S. 2018. Removal of sulfate from waste water by activated carbon. *Al-Khwarizmi Engineering Journal*, 5(3), 72-79.
- Santos, A. F. M., Macedo, L. J. A., Chaves, M. H., Espinoza-Castañeda, M., Merkoçi, A., Lima, F. et al. 2016. Hybrid self-assembled materials constituted by ferromagnetic nanoparticles and tannic acid: a theoretical and experimental investigation. *Journal of the Brazilian Chemical Society*, 27(4), 727-734.
- Mohamadi, A. S., Sarkhosh, M., Atafar, Z., Nazari, SH., Rezaei, S., Sheikh, A. et al. 2016. Removal of malachite green, a hazardous dye using graphene oxide as an adsorbent from aqueous phase. *Journal of Chemical and Pharmaceutical Research*, 8(3), 624-633.
- Shahbazi, A., Younesi, H. & Badiei, A. 2013. Batch and fixed-bed column adsorption of Cu (II), Pb (II) and Cd (II) from aqueous solution onto functionalised SBA-15 mesoporous silica. *The Canadian Journal of Chemical Engineering*, 91(4), 739-750.
- Shirsath, D. S. & Shirivastava, V. S. 2015. Adsorptive removal of heavy metals by magnetic nanoadsorbent: an equilibrium and thermodynamic study. *Applied Nanoscience*, 5(8), 927-935.
- Srivastava, S., Sinha, R. & Roy, D. 2004. Toxicological effects of malachite green. *Aquatic Toxicology*, 66(3), 319-329.
- Srivastava, V. C., Mall, I. D. & Mishra, I. M. 2008. Removal of cadmium (II) and zinc (II) metal ions from binary aqueous solution by rice husk ash. *Colloids and Surfaces A: Physicochemical and Engineering Aspects*. 312(2), 172-184.
- Tchobanoglous, G. & Burton, F. L. 1991. *Wastewater engineering, disposal and reuse*. Metcalf & Eddy'. INC.
- Vazquez, G., Gonzalez-Alvarez, J., Freire, S., López-Lorenzo, M. & Antorrena, G. 2002. Removal of cadmium and mercury ions from aqueous solution by sorption on treated Pinus pinaster bark: kinetics and isotherms. *Bioresource Technology*. 82(3), 247-251.
- Wang, Y., Li, Z., Hu, D., Lin, C. T., Li, J. & Lin, Y. 2010. Aptamer/graphene oxide nanocomplex for in situ molecular probing in living cells. *Journal of the American Chemical Society*, 132(27), 9274-9276.

